



ELSEVIER

Catalysis Today 44 (1998) 17–26



Recent progress of photocatalysts for overall water splitting

Tsuyoshi Takata^a, Akira Tanaka^b, Michikazu Hara^a, Junko N. Kondo^a, Kazunari Domen^{a,*}

^aResearch Laboratory of Resources Utilization, Tokyo Institute of Technology, 4259 Nagatsuta, Midori-ku, Yokohama 226, Japan

^bNikon Corp. 1-10-1 Asamizodai, Sagami-hara, Japan

Abstract

Recent progress of photocatalysts for H₂O decomposition into H₂ and O₂ was briefly reviewed with the emphasis on the results concerning the use of several ion-exchangeable layered materials. Very recent results concerned with the first successful example of overall water splitting induced by visible light irradiation was also presented. © 1998 Elsevier Science B.V. All rights reserved.

Keywords: Photocatalyst; Overall water splitting; Ion-exchangeable layered material

1. Introduction

Various kinds of photon energy conversion systems have been extensively studied from the viewpoint of solar energy utilization. Photocatalytic decomposition of H₂O into H₂ and O₂ is one of such systems in which clean and high energy-containing H₂ is directly obtained.

Since the report of Fujishima and Honda [1] using a TiO₂ photoelectrode in 1972, a lot of studies have been made in the field of photoelectrochemistry as well as photocatalysis. At the initial stage of the studies of photocatalytic decomposition of H₂O, simultaneous evolution of H₂ and O₂ using homogeneous or heterogeneous systems had not been well demonstrated mainly due to the difficulty of O₂ formation and to rapid reverse reaction between products. However, for the past decade, several heterogeneous photocatalytic systems have been remarkably developed to decom-

pose H₂O into H₂ and O₂ steadily under ultraviolet light irradiation [2–6], and a lot of useful knowledge on such an up-hill reaction have been accumulated. These heterogeneous photocatalysts typically consist of oxide powders mainly based on titanates and niobates with loading of certain metal or metal oxide such as NiO_x, RuO₂, RhO_x or Pt [2–8]. In this short review, recent developments accomplished by the authors and some other groups are introduced.

2. Photocatalyst with a tunnel structure

Inoue et al. [4] have reported an efficient overall water splitting on RuO₂-loaded BaTi₄O₉ catalyst [4]. The main feature in the structure of BaTi₄O₉ is the pentagonal-prism tunnel structure. It is suggested that the distorted TiO₆ octahedra in pentagonal-prism tunnel structure is essential for an efficient H₂O decomposition. The distorted TiO₆ octahedron generates dipole moments, which efficiently work for the separation of photogenerated charges. Furthermore,

*Corresponding author. Tel.: 81 45 924 5238; fax: 81 45 924 5276; e-mail: kdomen@res.titech.ac.jp

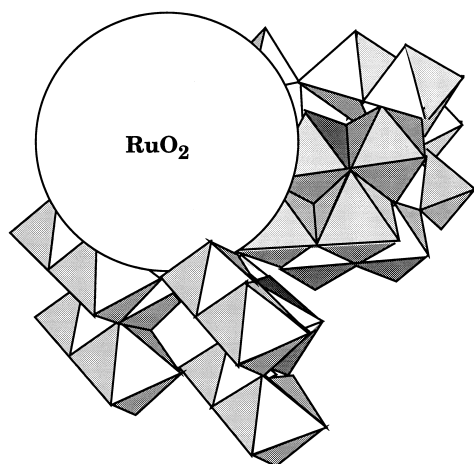


Fig. 1. Schematic illustration of the model of a 'nest' effect of a pentagonal-prism tunnel in the $\text{RuO}_2\text{-BaTi}_4\text{O}_{19}$ photocatalyst.

the tunnel structure serves the uniform distribution of RuO_2 particles. The pentagonal-prism tunnel space provides the form of a 'nest', i.e., a concave site with a ridge in which a small RuO_2 particle firmly accommodates as depicted in Fig. 1. The strong interaction between the small RuO_2 particle and the surrounding TiO_6 octahedra facilitates the transfer of photoexcited electrons and holes to the adsorbed species.

3. Effect of carbonate anion on overall water splitting

An interesting and useful effect on overall water splitting concerning the reaction solution has been reported by Sayama and Arakawa [5,9–11]. It is well known that Pt-TiO_2 , a typical photocatalyst, cannot decompose water in an aqueous solution because of the rapid reverse reaction on the loaded Pt. However, Sayama and Arakawa found that in a concentrated Na_2CO_3 solution, H_2 and O_2 evolve efficiently. This suggests that the reverse reaction is suppressed in the solution. They further proposed that adsorbed CO_3^{2-} ions on to the catalyst enhanced the O_2 evolution through the formation of peroxycarbonates in addition to the prevention of reverse reaction on Pt. The significance of this finding is the wide applicability to various photocatalytic systems. Table 1 summarizes

some of those examples. They also demonstrated the H_2 and O_2 evolutions on $\text{NiO}_x\text{-TiO}_2$ in Na_2CO_3 aqueous solution under solar light irradiation.

4. An ion-exchangeable layered niobate, $\text{A}_4\text{Nb}_6\text{O}_{17}$ ($\text{A}=\text{K}, \text{Rb}$), for overall water splitting

We have reported that the application of some ion-exchangeable layered oxides to overall water splitting is advantageous in several respects as compared with the so-called "bulk type" photocatalysts represented by TiO_2 . One of the advantages of using layered materials as photocatalysts is the availability of inter-layer space as reaction sites [6,12–15]. In practice, Ni-modified $\text{A}_4\text{Nb}_6\text{O}_{17}$ ($\text{A}=\text{K}, \text{Rb}$) catalysts exhibit steady evolution of H_2 and O_2 at high quantum efficiencies under ultraviolet light irradiation [6,13].

$\text{K}_4\text{Nb}_6\text{O}_{17}$ consists of NbO_6 octahedron units which form a two-dimensional layered structure via oxygen atoms. These layers have negative charges, and positively charged K^+ ions exist between layers in order to keep a balance with the negative charges of the layers. The most peculiar feature in the structures of $\text{K}_4\text{Nb}_6\text{O}_{17}$ is alternately appearing two types of inter-layer space, i.e., interlayer I and II. The two types of interlayer space exhibit different ion-exchange properties from each other. K^+ ions at the interlayer space I are able to be replaced by Li^+ , Na^+ and some multi-valent cations while those at the interlayer space II are replaced only by monovalent cations such as Li^+ and Na^+ . The other characteristic to be noted in the structure of $\text{K}_4\text{Nb}_6\text{O}_{17}$ is the spontaneous hydration of the interlayer space. This material is easily hydrated in a highly humid air as well as in an aqueous solution. This indicates that the reactant, H_2O molecules, are easily intercalated into the interlayer space during the photocatalytic reaction.

$\text{K}_4\text{Nb}_6\text{O}_{17}$ alone in distilled water evolved H_2 and O_2 under the band gap (ca. 3.3 eV) irradiation although the amount of O_2 evolved was considerably less than the stoichiometry. Marked enhancement in activity of H_2O decomposition was observed when the catalyst was modified by Ni. The modifications of the catalyst by other metals or metal oxides did not affect the increase in photocatalytic activity. The Ni-loading led to decomposition of H_2O into H_2 and O_2 steadily

Table 1

Photocatalytic decomposition of water over various catalysts in both aqueous Na₂CO₃ solution and distilled water

Catalyst	Loaded materials	Rate of gas evolution ($\mu\text{mol h}^{-1}$)			
		Na ₂ CO ₃ solution		Distilled water	
		H ₂	O ₂	H ₂	O ₂
TiO ₂	None	Trace	0	Trace	0
	Pt (0.3 wt%)	78	38	2	0
	RuO ₂ (1 wt%)	34	17	Trace	0
	NiO _x (1 wt%)	64	32	1	0
Ta ₂ O ₅	None	Trace	0	Trace	0
	Pt (0.1 wt%)	1	0	1	0
	RuO ₂ (1 wt%)	68	34	32	17
	NiO _x (1 wt%)	153	79	190	99
ZrO ₂	None	142	75	72	36
	Pt (0.1 wt%)	53	23	Trace	0
	RuO ₂ (1 wt%)	12	6	11	5
	NiO _x (1 wt%)	43	22	129	70
SrTiO ₃	None	Trace	0	Trace	0
	Pt (1 wt%)	10	4	9	2
	Rh (0.1 wt%)	48	14	20	4
	NiO _x (1 wt%)	41	20	9	4
K ₄ Nb ₆ O ₁₇	Pt (0.3 wt%) ^a	451	217	Trace	0
	NiO _x (1 wt%)	60	28	403	197
	RuO ₂ (1 wt%)	41	20	211	100
Na ₂ Ti ₆ O ₁₃	Pt (1 wt%)	15	5	Trace	0
	RuO ₂ (1 wt%)	55	25	5	2
K ₂ Ti ₆ O ₁₃	Pt (0.1 wt%)	63	17	Trace	0
	RuO ₂ (1 wt%)	49	24	11	1
BaTi ₄ O ₉	Pt (0.1 wt%)	2	Trace	Trace	0
	RuO ₂ (1 wt%)	36	18	30	13

Catalyst, 1.0 g; solution, 350 ml; inner irradiation-type quartz reaction cell; high pressure Hg lamp (400 W); Na₂CO₃, 80 g.^aPrecursor of Pt, [Pt(NH₃)₄]Cl₂, without aqua regia treatment.

and efficiently after the pretreatment of H₂ reduction at 773 K for 2 h followed by reoxidation in O₂ at 473 K for 1 h (referred to as R773–O473). The highest activity was obtained over Ni(0.1 wt%)–K₄Nb₆O₁₇ with R773–O473 treatment when the reaction was carried out in distilled water, and the time course of H₂ and O₂ evolution under the irradiation with a high pressure Hg lamp is shown in Fig. 2. A similar result was obtained for Rb₄Nb₆O₁₇, in which higher quantum efficiency (ca. 10% at 330 nm) than that of K₄Nb₆O₁₇ (ca. 5% at 330 nm) was obtained.

From the structural studies by means of XPS, TEM and EXAFS, the structure of active Ni(0.1 wt%)–K₄Nb₆O₁₇ catalyst was elucidated. Most of the loaded nickel was located in the interlayer I as metallic ultrafine particles (ca. 5 Å) after the R773–O473 treatment. On the bases of the structure of active Ni–K₄Nb₆O₁₇ catalyst, reaction mechanism of H₂O decomposition was suggested as follows. The active sites for H₂ evolution are on the Ni metal ultrafine particles at the interlayer space I, and the active sites for O₂ evolution are in the interlayer space II.

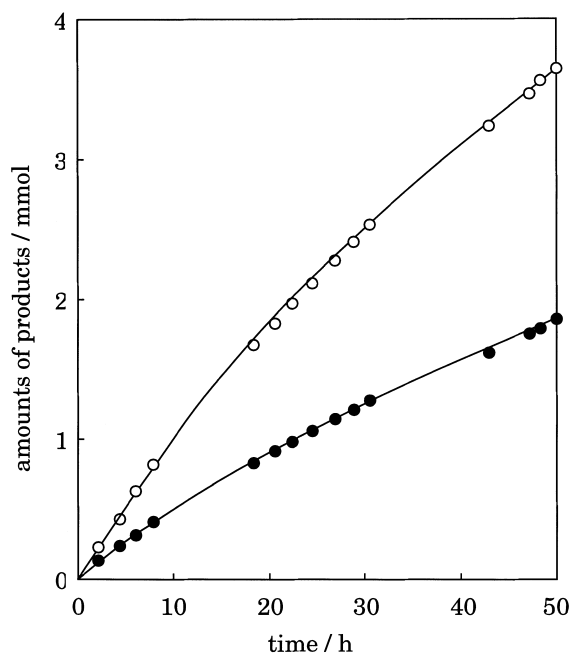


Fig. 2. Time course of H₂ and O₂ evolution over Ni(0.1 wt%)-K₄Nb₆O₁₇ catalyst from distilled water. Open circle, H₂; closed circle, O₂; catalyst, 1.0 g; H₂O, 350 ml; high pressure Hg lamp (450 W); inner irradiation-type pyrex reaction cell.

A₄Nb₆O₁₇ (A=K, Rb) absorbs photons only in the ultraviolet region. Several attempts to extend the absorption edge into visible region were carried out, but none of them were successful so far. We, therefore, surveyed several other types of layered materials for H₂O decomposition. As a result, it has been revealed that layered perovskites are the promising materials for H₂O decomposition, which is presented in the next section.

5. Application of ion-exchangeable layered perovskites as photocatalysts to water splitting

Here, we describe the photocatalytic behaviors of a series of layered perovskite type niobates with a general formula of A[M_{n-1}Nb_nO_{3n+1}] (A=K, Rb, Cs; M=Ca, Sr, Na, Pb, etc.; n=2–4) [14]. These materials consist of interlayer alkaline metal cations and negatively charged mixed oxide sheets with a perovskite structure stacking along the *c*-axis as illustrated in Fig. 3. ALaNb₂O₇ and KCa₂Nb₃O₁₀ are the

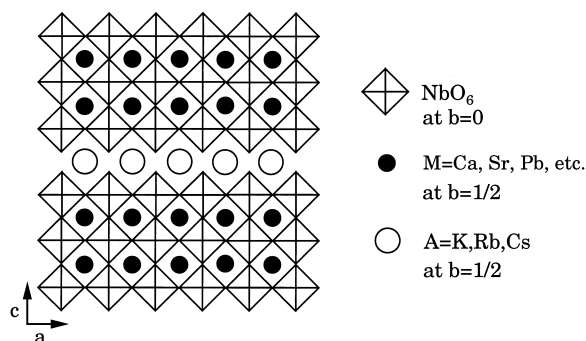


Fig. 3. Schematic structure of A[M_{n-1}Nb_nO_{3n+1}] (n=3).

members of n=2 and 3, respectively. Band gaps estimated from UV–vis diffuse reflectance spectra are 3.2–3.5 eV for all catalysts. These layered perovskites are not hydrated in the original forms. However, they become hydrated by substituting the interlayer alkaline metal cations by protons. Since simultaneous evolution of H₂ and O₂ was not attained even with several modified catalysts, the photocatalytic activities of these catalysts were evaluated from the following two reactions containing sacrificial reagents; photocatalytic H₂ evolution from aqueous methanol solution and O₂ evolution from aqueous silver nitrate solution.

Rates of photocatalytic evolution of H₂ or O₂ are summarized in Table 2 for all the layered perovskites as well as their H⁺-exchanged derivatives under the irradiation with a high pressure Hg lamp. The original forms of all layered perovskites evolve H₂ without any modification, and the rates of H₂ evolution are enhanced by several times with Pt-loading in each case. Furthermore, marked enhancement of the rate of H₂ evolution by about two or three orders of magnitude is attained by the substitution of protons for interlayer alkaline metal cations. As is mentioned above, these layered perovskites become hydrated by the H⁺-replacement, and accordingly, migration of reactants also become possible for H⁺-exchanged derivatives. Therefore, it is inferred that the marked enhancement of H₂ evolution which was brought about by the H⁺-replacement is attributed to the availability of the interlayer space as reaction sites.

To confirm the above speculation, the relationship between migration of reactants and the rate of H₂ evolution was examined. In Table 3, the rates of H₂

Table 2

Photocatalytic activities of layered perovskite compounds $A[M_{n-1}Nb_nO_{3n-1}]$

Catalyst	<i>n</i>	Rate of gas evolution (μmol h ^{−1})				O ₂ ^b
		H ₂ ^a				
		Original		H ⁺ -exchanged ^c		
		Alone	Pt-loaded ^d	Alone	Pt-loaded ^d	
KLaNb ₂ O ₇	2	28	54	760	3800	46
RbLaNb ₂ O ₇	2	60	90	740	2600	2
CsLaNb ₂ O ₇	2	12	28	300	2200	3
Ksa ₂ Nb ₃ O ₁₀	3	14	100	5900	19 000	8
RbCa ₂ Nb ₃ O ₁₀	3	3	26	3100	1700	16
CsCa ₂ Nb ₃ O ₁₀	3	2	10	970	8300	10
KSr ₂ Nb ₃ O ₁₀	3	10	110	8900	43 000	30
KCa ₂ NaNb ₄ O ₁₃	4	5	280	790	18 000	39

Catalyst 1.0 g, high pressure Hg lamp (450 W).

^aMeOH 50 ml+H₂O 300 ml.^b0.01 M AgNO₃ aq. 350 ml.^cH⁺-exchange degree >95%.^dPt was loaded from H₂PtCl₆ aq. by photodeposition method. The amounts of loading were 0.1 wt%.

Table 3

Rate of H₂ evolution from various alcohol solutions ($\mu\text{mol h}^{-1}$)

Alcohol	Catalyst		
	$\text{KCa}_2\text{Nb}_3\text{O}_{10}$	$\text{Pt-H}^+/\text{KCa}_2\text{Nb}_3\text{O}_{10}^{\text{a,b}}$	Pt-TiO_2^b
Methanol	7	4670	4000
Ethanol	7	384	5170
1-Propanol	3	43	3480
1-Butanol	2	30	2790

Catalyst, 1.0 g solution, alcohol 50 ml+H₂O 300 ml; Hg lamp (450 W).^aH⁺-exchange degree >95%.^b0.1 wt% of Pt loading.

evolution from various alcohol solutions over H⁺-exchanged $\text{KCa}_2\text{Nb}_3\text{O}_{10}$ catalyst are compared. With the increase of the length of carbon chain of alcohols from methyl to butyl, the rate of H₂ evolution decreased by more than two orders of magnitude, which is in distinct contrast to the cases of original $\text{KCa}_2\text{Nb}_3\text{O}_{10}$ and Pt-TiO₂ catalysts shown for comparison. This result supports that the migration of reactants into the interlayer space determines the reaction rate.

In aqueous silver nitrate solution, O₂ evolution was observed for each catalyst as shown in Table 2. It is, therefore, suggested that these layered perovskites have a potential for overall water splitting as in the

case of $\text{A}_4\text{Nb}_6\text{O}_{17}$ if any proper modifications are made. It is further noted that this type of layered perovskites have many relatives, and that some of them show photoresponse in visible light region; $\text{RbPb}_2\text{Nb}_3\text{O}_{10}$ is one of such materials [15]. This material is also not hydrated in the original form while it is hydrated by the substitution of protons for inter-layer Rb⁺ ions. The absorption edge of $\text{RbPb}_2\text{Nb}_3\text{O}_{10}$ extends to about 500 nm.

The rates of photocatalytic evolution of H₂ on several $\text{RbPb}_2\text{Nb}_3\text{O}_{10}$ -based catalysts from aqueous methanol solution under the irradiation with a Xe-lamp through a cut-off filter (>420 nm) are summarized in Table 4. $\text{RbPb}_2\text{Nb}_3\text{O}_{10}$ alone or Pt-loaded $\text{RbPb}_2\text{Nb}_3\text{O}_{10}$ showed almost negligible activities of H₂ evolution. However, marked increase of H₂ evolution was observed for their H⁺-exchanged forms (referred to as $\text{HPb}_2\text{Nb}_3\text{O}_{10}$). As is suggested above, the migration of reactants are possible for H⁺-exchanged form.

Further enhancement of activity was obtained by an improvement of Pt-loading method. Pt was loaded by in situ photodeposition method in H₂PtCl₆ aqueous solution in the cases of the reaction shown in Table 4. Since this Pt precursor is an anion of PtCl_6^{2-} and cannot be intercalated into the interlayer space of $\text{HPb}_2\text{Nb}_3\text{O}_{10}$, a cation exchanger, Pt should be depos-

Table 4

Photocatalytic activities of several modified $\text{RbPb}_2\text{Nb}_3\text{O}_{10}$ catalysts

Catalyst	Rate of gas evolution ($\mu\text{mol h}^{-1}$)		
	H_2^{a}		O_2^{b}
	Alone	Pt-loaded ^c	
Original	0	0.1	1.1
H^+ -exchanged	0.59	3.7	0

Catalyst 1.0 g; 500 W Xe lamp (>420 nm).

^a H_2O (25 ml)+methanol (50 ml).

^b0.01 M AgNO_3 aq. (250 ml).

^cPt was loaded from H_2PtCl_6 aq. by photodeposition method. The amounts of loading were 0.1 wt%.

ited on the external surface of the catalyst. Thus, photoexcited electrons in the bulk of the catalyst should migrate to the external Pt particles in order to efficiently reduce protons and to evolve H_2 . During the migration of electrons, some of them should be consumed by the recombination with the simultaneously generated holes. For the purpose of decreasing recombination of photogenerated electrons and holes, Pt was dispersed into the catalyst by an ion-exchange using $[\text{Pt}(\text{NH}_3)_4]\text{Cl}_2$ as a precursor in which $\text{Pt}(\text{NH}_3)_4^{2+}$ cations exist in an aqueous solution. In Fig. 4, the rates of H_2 evolution were presented as a function of the period of ion-exchange treatment of $\text{HPb}_2\text{Nb}_3\text{O}_{10}$ in an aqueous solution containing $\text{Pt}(\text{NH}_3)_4^{2+}$. The rate of H_2 evolution increased with increasing ion-exchange time and reached maximum after a week. On the other hand, no effect of the treatment time on the H_2 evolution rate was observed for the catalyst loaded from H_2PtCl_6 . The marked increase in the rate of H_2 evolution is attributed to the existence of Pt particles adjacent to the excited electrons.

It is another interesting question whether this catalyst evolves O_2 under visible light irradiation. Constant rate of O_2 evolution ($1.1 \mu\text{mol h}^{-1}$) from aqueous silver nitrate solution was observed for original $\text{RbPb}_2\text{Nb}_3\text{O}_{10}$ while no O_2 evolution was observed for $\text{HPb}_2\text{Nb}_3\text{O}_{10}$ as shown in Table 4. The deficiency of O_2 evolution in the case of $\text{HPb}_2\text{Nb}_3\text{O}_{10}$ may be due to the acidic property of the interlayer space which suppresses the O_2 formation.

As it turned out from the above results, a series of layered perovskite type niobate, $\text{A}[\text{M}_{n-1}\text{Nb}_n\text{O}_{3n+1}]$

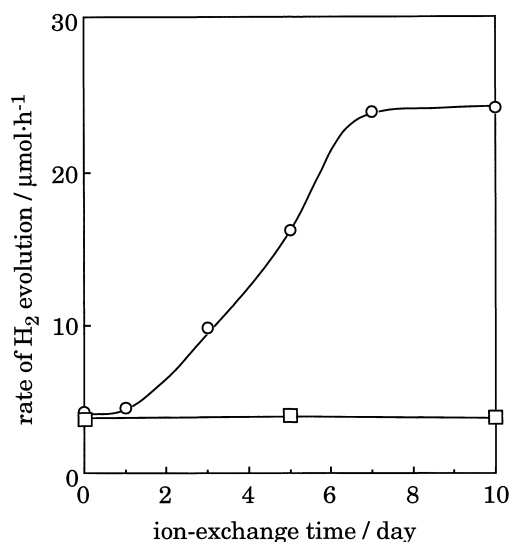


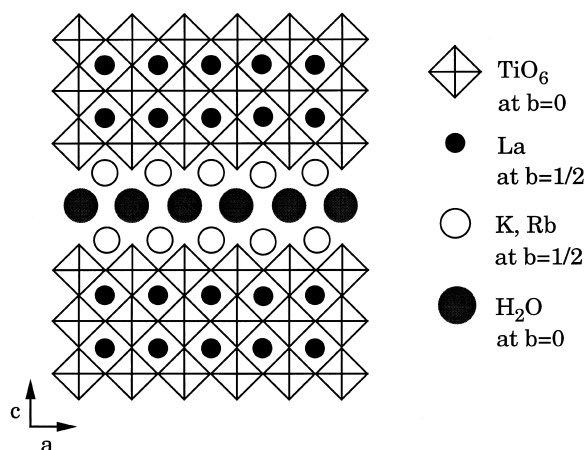
Fig. 4. Rate of H_2 evolution as a function of the treatment time of $\text{RbPb}_2\text{Nb}_3\text{O}_{10}$ in an aqueous solution containing a Pt precursor. Open circle, $[\text{Pt}(\text{NH}_3)_4]\text{Cl}_2$; open square, H_2PtCl_6 ; Pt(0.1 wt%) fixed on the catalyst; Xe lamp 500 W (>420 nm); catalyst 1.0 g; solution, methanol (50 ml)+ H_2O (250 ml).

($\text{A}=\text{K}, \text{Rb}, \text{Cs}$; $\text{M}=\text{Ca}, \text{Sr}, \text{Pb}$, etc.; $n=2-4$) could be a highly active photocatalyst. However, an alkaline condition is usually preferred or indispensable for the decomposition of H_2O into H_2 and O_2 [16,17], and the above-examined layered perovskites are not hydrated in such an alkaline condition. The absence of hydration in an alkaline condition would be one of the reasons for the failure in an overall water splitting for the niobates.

6. Spontaneously hydrated layered perovskites

Next, we describe the use of a series of ion-exchangeable layered perovskites with a general formula of $\text{A}_{2-x}\text{La}_2\text{Ti}_{3-x}\text{Nb}_x\text{O}_{10}$ ($\text{A}=\text{K}, \text{Rb}, \text{Cs}$; $x=0, 0.5, 1.0$) as a successful example of efficient overall water splitting [18,19].

The structure of $\text{A}_2\text{La}_2\text{Ti}_3\text{O}_{10}$ ($\text{A}=\text{K}, \text{Rb}$) is schematically depicted in Fig. 5. $\text{A}_{2-x}\text{La}_2\text{Ti}_{3-x}\text{Nb}_x\text{O}_{10}$ substances also consist of interlayer alkaline metal cations and of negatively charged two-dimensional sheets composed of mixed oxides with a perovskite type structure. One of the characteristics in the struc-

Fig. 5. Schematic structure of A₂La₂Ti₃O₁₀ (A=K, Rb).

ture of A₂La₂Ti₃O₁₀ is spontaneous hydration of the interlayer space, which is a clear difference from the above-described layered perovskite niobates. Band gaps estimated from UV–vis diffuse reflectance spectra are 3.4–3.5 eV for all catalysts.

In Table 5, the numbers of hydration and the optimum activities as well as their conditions (amount of loaded nickel and pH value of the solution) for all the catalysts are summarized. Rb₂La₂Ti₃O₁₀ with 4.0 wt% of Ni-loading in aqueous RbOH solution (0.1 M, pH=12.8) showed the highest activity of all the catalysts examined. Typical time courses of H₂ and O₂ evolution on Ni-modified K₂La₂Ti₃O₁₀ and Rb₂La₂Ti₃O₁₀ catalysts under the irradiation with a high pressure Hg lamp are shown in Fig. 6. Constant rates of H₂ and O₂ evolution at almost stoichiometric

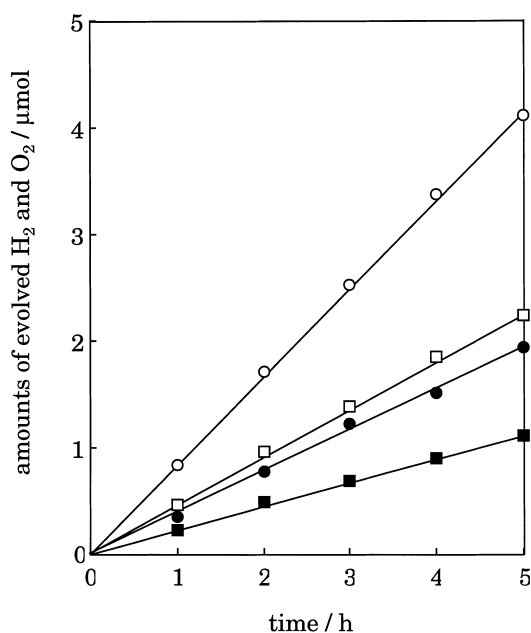


Fig. 6. Typical time courses of H₂ and O₂ evolution over nickel-loaded layered perovskites. Open circle, H₂; filled circle, O₂, Ni(4.0 wt%)-Rb₂La₂Ti₃O₁₀ (1.0 g) in aqueous RbOH solution (0.1 M); open square, H₂; filled square, O₂, Ni(3.0 wt%)-K₂La₂Ti₃O₁₀ (1.0 g) in aqueous KOH solution (0.1 M); catalyst, 1.0 g; solution, 330 ml; high pressure Hg lamp (450 W); inner irradiation-type quartz reaction cell.

ratio were observed for both catalysts. The pretreatment of R773–O473 was also indispensable to evolve H₂ and O₂ steadily and efficiently.

The interlayer space was not hydrated when one-third of Ti⁴⁺ was replaced by Nb⁵⁺ although

Table 5
Photocatalytic activities of various layered perovskites and hydration numbers

Catalyst	Rate of gas evolution (μmol h ⁻¹) ^a		Optimum condition		Hydration number (n) ^c
	H ₂	O ₂	Ni-loading (wt%) ^b	pH	
K ₂ La ₂ Ti ₃ O ₁₀	444	221	3.0	12.8	1.0
Rb ₂ La ₂ Ti ₃ O ₁₀	869	430	4.0	12.8	1.1
Rb _{1.5} La ₂ Ti _{2.5} Nb _{0.5} O ₁₀	725	358	5.0	12.6	0.9
RbLa ₂ Ti ₂ NbO ₁₀	79	30	0.3	12.8	0
CsLa ₂ Ti ₂ NbO ₁₀	115	50	0.3	8.5	0

^aCatalyst, 1.0 g; H₂O, 330 ml; high pressure Hg lamp (450 W); an inner irradiation-type quartz reaction cell.

^bAmount of loaded Ni.

^cThe number of hydration in the formula of A_{2-x}La₂Ti_{3-x}Nb_xO₁₀·nH₂O.

hydration took place for $\text{A}_2\text{La}_2\text{Ti}_3\text{O}_{10}$ and $\text{A}_{1.5}\text{La}_2\text{Ti}_{2.5}\text{Nb}_{0.5}\text{O}_{10}$ as seen from Table 4. The activity of $\text{ALa}_2\text{Ti}_2\text{NbO}_{10}$ catalyst was lower by about an order of magnitude than the others while there is no evident difference in activity between $\text{A}_2\text{La}_2\text{Ti}_3\text{O}_{10}$ and $\text{A}_{1.5}\text{La}_2\text{Ti}_{2.5}\text{Nb}_{0.5}\text{O}_{10}$ catalysts. It is inferred that the lower activity of $\text{ALa}_2\text{Ti}_2\text{NbO}_{10}$ catalyst is due to the absence of hydration. The absence of hydration in the case of $\text{ALa}_2\text{Ti}_2\text{NbO}_{10}$ is attributed to the structural transformation caused by the Nb^{5+} replacement. By increasing the amount of Nb in the layers, the number of alkaline metal cations held in the interlayer space decreases in order to maintain the charge balance between the layers and interlayers. $\text{ALa}_2\text{Ti}_2\text{NbO}_{10}$ is isostructural with a series of layered perovskite, $\text{A}[\text{M}_{n-1}\text{Nb}_n\text{O}_{3n+1}]$, which was described above, and $\text{A}[\text{M}_{n-1}\text{Nb}_n\text{O}_{3n+1}]$ series are not hydrated without exception. It seems that layered perovskites which hold larger amount of alkaline metal cations at the interlayer space are easily hydrated. The increase of the negative charge density enables to increase the amount of alkaline metal cations at the interlayer space. This indicates a useful guiding principle to develop photocatalysts for an efficient water splitting with a hydrated layered perovskite type structure.

7. Visible light induced photocatalytic overall water splitting on CuFeO_2 with delafossite structure

As presented in the preceding sections, an efficient overall water splitting has been accomplished on properly modified photocatalysts under ultraviolet light irradiation. However, an overall water splitting under visible light irradiation has not been attained on such photocatalysts. The materials successfully used for an overall water splitting have been dominated by the oxides containing early transition metal cations with d^0 electronic configuration such as Ti^{4+} , Nb^{5+} , Ta^{5+} and Zr^{4+} . These materials generally have wide band gaps (>3.0 eV) and do not work under visible light irradiation. Although several attempts have been made to use the oxides containing other transition metal cations as photocatalyst for water splitting, unsuccessful results have not attracted much attention.

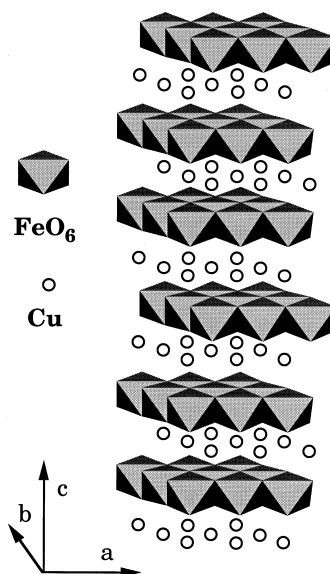


Fig. 7. Schematic structure of CuFeO_2 .

Some of Cu^+ -containing oxides such as Cu_2O seem to have suitable electronic band structures for water decomposition under visible light irradiation [20]. The major problem of these materials as photocatalysts is the instability of oxides against irradiation in an aqueous solution. However, we have found very recently that some Cu^+ -containing delafossites evolve H_2 and O_2 under visible light irradiation when they are suspended in distilled water.

The schematic structure of the delafossite, CuFeO_2 , is shown in Fig. 7 [21]. The basic formula is $\text{Cu}^{1+}\text{Fe}^{3+}\text{O}_2$, with Cu^{1+} in a linear coordination with oxygen, and Fe^{3+} in an octahedral coordination. The FeO_6 octahedra share edges to form a triangular plane analogous to what is observed in octahedrally coordinated transition metal dichalcogenides such as MoS_2 .

Typical time course of H_2 and O_2 evolution over CuFeO_2 catalyst (0.5 g) in distilled water (250 ml) under the irradiation with a Xe lamp through a cut-off filter (>420 nm) is shown in Fig. 8. The reaction continued for about 1800 h with evacuation at about every 300 h (the full time course is not shown in Fig. 8), and the total amounts of evolved H_2 and O_2 reached 1720 and 520 μmol , respectively. The amount of the catalyst used was 3300 μmol of CuFeO_2 .

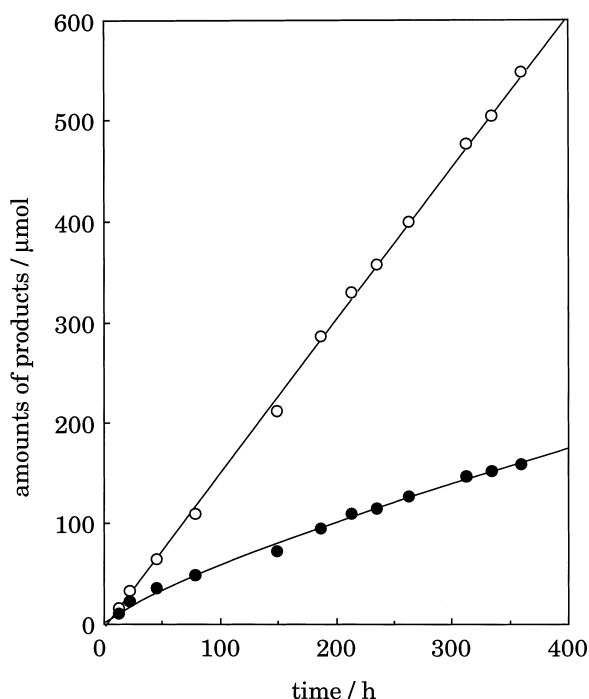


Fig. 8. Time courses of H₂ and O₂ evolution on CuFeO₂ under visible light irradiation. The full time course of 1800 h is not shown. Open circle, H₂; closed circle, O₂; catalyst, 0.5 g; H₂O, 250 ml; 500 W Xe lamp (>420 nm).

Assuming that two electrons per H₂ molecule evolved are consumed, the number of electrons exceeded that of Cu⁺ or Fe³⁺ in the used CuFeO₂. The crystal structure of the catalyst after the reaction for 1800 h was essentially the same as that before the reaction so far as observed by the X-ray diffraction patterns. These results confirmed the catalytic cycle of this system. The shortage of O₂ evolution less than the stoichiometry seems to be due to the oxidation of Cu¹⁺ to Cu²⁺ which is probably the reason for the suppression of the activity as observed in the long reaction time.

The delafossite type oxide, CuFeO₂, has the linear O–Cu⁺–O arrays, in which valence and conduction bands are formed primarily by the Cu-2p and O-2p wave functions [22]. If the linear O–Cu⁺–O array is essential for the observed water splitting, other materials having similar structures are expected to show the response for visible light irradiation. Those materials are now under investigation in our group, and some of

them have actually been found to show similar photocatalytic behaviors.

8. Summary and prospect

An efficient overall water splitting under ultraviolet light irradiation has already been accomplished on various photocatalysts including ion-exchangeable layered materials with proper modifications. Especially for the layered photocatalysts, it has also been demonstrated that the use of interlayer space as reaction sites is effective to obtain high activity of water splitting. Furthermore, an overall water splitting under visible light irradiation has, for the first time, been successfully accomplished using a novel catalyst, CuFeO₂, with delafossite structure although the quantum efficiency has yet been low (0.05–0.1%). One of the reasons for the low efficiency may be that H₂O molecules are decomposed only on the external surface of the catalyst. If CuFeO₂ or CuFeO₂-based catalysts are modified to have large surface area available for H₂O decomposition as in the case of hydrated layered materials, marked enhancement of activity of H₂O decomposition would be expected. Main efforts of our study are now focused in this direction.

References

- [1] A. Fujisima, K. Honda, *Nature* 37 (1972) 238.
- [2] K. Domen, A. Kudo, T. Onishi, *J. Catal.* 102 (1986) 92.
- [3] Y. Inoue, T. Kubokawa, K. Sato, *J. Phys. Chem.* 95 (1991) 4059.
- [4] Y. Inoue, Y. Asai, K. Sato, *J. Chem. Soc., Faraday Trans.* 90 (1994) 792.
- [5] K. Sayama, H. Arakawa, *J. Photochem. Photobiol. A* 77 (1994) 243.
- [6] A. Kudo, K. Domen, K. Maruya, K. Aika, T. Onishi, *J. Catal.* 111 (1988) 67.
- [7] J.M. Lehn, J.P. Sauvage, R. Ziessel, *Nouv. J. Chim.* 4 (1980) 623.
- [8] K. Sayama, H. Arakawa, K. Domen, *Catal. Today* 28 (1996) 175.
- [9] K. Sayama, H. Arakawa, *J. Chem. Soc., Chem. Commun.* (1992) 450.
- [10] K. Sayama, H. Arakawa, *Chem. Lett.* (1992) 253.
- [11] K. Sayama, H. Arakawa, *J. Phys. Chem.* 97 (1993) 531.
- [12] A. Kudo, K. Sayama, A. Tanaka, K. Asakura, K. Domen, K. Maruya, T. Onishi, *J. Catal.* 120 (1989) 337.

- [13] K. Sayama, A. Tanaka, K. Domen, K. Maruya, T. Onishi, *J. Catal.* 124 (1990) 541.
- [14] K. Domen, J. Yoshimura, T. Sekine, A. Tanaka, T. Onishi, *Catal. Lett.* 4 (1990) 339.
- [15] J. Yoshimura, Y. Ebina, J. Kondo, K. Domen, *J. Phys. Chem.* 97 (1993) 1970.
- [16] K. Domen, S. Naito, T. Onishi, K. Tamaru, *Chem. Phys. Lett.* 92 (1982) 433.
- [17] A. Kudo, K. Domen, K. Maruya, T. Onishi, *Chem. Phys. Lett.* 133 (1987) 517.
- [18] T. Takata, K. Shinohara, A. Tanaka, M. Hara, J.N. Kondo, K. Domen, *J. Photochem. Photobiol. A* 106 (1997) 45.
- [19] T. Takata, Y. Furumi, K. Shinohara, A. Tanaka, M. Hara, J.N. Kondo, K. Domen, *Chem. Mater.* 9 (1997) 1063.
- [20] H. Gerischer, *J. Electroanal. Chem.* 82 (1977) 133.
- [21] R.D. Shannon, D.B. Rogers, C.T. Prewitt, *Inorg. Chem.* 10 (1971) 713.
- [22] D.B. Rogers, R.D. Shannon, C.T. Prewitt, J.L. Gillson, *Inorg. Chem.* 10 (1971) 723.